Engineering Structures 52 (2013) 581–591

Contents lists available at SciVerse ScienceDirect

Engineering Structures

journal homepage: www.elsevier.com/locate/engstruct

Testing and modeling the diagonal tension strength of rubble stone masonry panels

Jelena Milosevic *, Mário Lopes, António Sousa Gago, Rita Bento

ICIST, IST, Technical University of Lisbon, Portugal

ARTICLE INFO

Article history:
Received 10 November 2012
Revised 24 December 2012
Accepted 12 March 2013

Keywords:
Masonry buildings
Shear strength
Experimental tests
Diagonal compression test
Earthquake
Finite element model
Distinct element model

ABSTRACT

The present paper deals with the experimental study performed by diagonal compression tests on four rubble stone masonry panels (120 cm × 120 cm × 70 cm) within the scope of the research project *SEVERES* aiming at characterizing the seismic behavior of old masonry buildings. In this research two types of mortar were used, namely two specimens were built with hydraulic lime and other two specimens were built with air lime mortar. The shear strength and the shear modulus of rubble stone panels were obtained. These results were compared with the values obtained by other authors and suggested by the Italian's standards. It is important to refer that the experimental research allowed characterizing the mechanical properties of masonry panels, which were built using traditional techniques in order to simulate old buildings in Portugal. Together with the experimental research, (additionally) numerical interpretation of the tests is also given in order to simulate the behavior of the panels.

1. Introduction

Many cities located in regions of intense seismic activity have a significant number of old masonry buildings. These buildings are occupied mainly by services and housing, and many have a not negligible architectural value. Therefore, to preserve the architectural heritage and decrease the seismic risk in those regions, structural studies should be conducted in order to decide where and how strengthening techniques should be used [1].

Lisbon is an area of intense seismic activity, where in 1755, one of the largest earthquakes in history destroyed the city and other towns in the south of Portugal. However, nowadays about 39% of the Lisbon building stock are old buildings built with masonry loadbearing walls and wooden floors, most with an inadequate seismic behavior. Two types of masonry buildings were built in Lisbon after 1755: (i) the so called "Pombalino" buildings [2,3], built in the decades after the earthquake, where specific construction techniques were adopted to enhance the buildings seismic behavior, and (ii) the buildings constructed during the expansion of the city at the late nineteenth and early 20th-century, known as "Gaioleiro" buildings [4], with lower construction quality. Despite the different construction techniques of these buildings, the constitution of their exterior walls is similar: thick rubble masonry walls with limestone and air lime mortar. This type of wall was widely used in the eighteenth and nineteenth centuries in Portugal and in all Mediterranean's countries.

For any numerical analysis it is important to know the mechanical characteristics of the constituent materials in order to simulate properly the buildings structural behavior. However, there are few studies where values for shear strength parameters of old masonry buildings can be found, which are actually a very relevant parameter for the evaluation of seismic behavior of masonry buildings.

The work described in this paper, developed under the framework of the research project *SEVERES* (www.severes.org), aims to characterize the seismic behavior of the aforementioned two types of buildings, including experimental tests for characterization of the shear strength of rubble stone masonry. These tests consist of diagonal compression tests (described in this paper), axial compression tests and shear tests (triplet and cyclic tests).

The diagonal compression tests followed, as close as possible, the test specifications of ASTM E519-02 standard [5] and similar works where rubble stone masonry panels were tested [6–12]. For these tests, four rubble stone masonry panels with dimensions of 120 cm × 120 cm × 70 cm were built (Fig. 1), with two types of mortar: two panels were built with hydraulic lime mortar and the other two with air lime mortar.

The diagonal compression tests were carried out to determine the shear strength of rubble stone masonry panels, the diagonal tensile strength and the shear modulus.

* Corresponding author. Address: IST DECivil – Av. Rovisco Pais, 1049-001 Lisboa, Portugal. Tel.: +351 927195525; fax: +351 218418200.
E-mail address: jelena.milosevic@ist.utl.pt (J. Milosevic).

0141-0296/$ - see front matter © 2013 Elsevier Ltd. All rights reserved.
http://dx.doi.org/10.1016/j.engstruct.2013.03.019

Fig. 1. Panels for diagonal compression tests.

Numerical analyses were also performed to reproduce the experimental tests. Based on experimental results nonlinear finite element models (smeared crack approach) and distinct element models were calibrated, by means of DIANA [13] and UDEC [14] computer's codes, respectively.

2. Characterization of masonry materials and construction of tests panels

The panels built for this experimental campaign are mainly characterized by roughly cut stone, in order to reproduce the common features of the traditional construction methodology. The stones were carefully chosen to secure theirs best application, leaving as few voids as possible. The dimensions of the stones varied and during the construction period, special attention was paid on choosing the larger stones (with the average dimension of the longest edge of 25 cm) as the basic building units, especially for the wall edges. The chosen stones are further locked together by applying the mortar and small stones in order to make the wall solid and stable.

The lime stones that were used to build the panels had the same origin and similar mechanical characteristics as the stones that were used by the old masons. Compression tests on this type of stones were done on a previous experimental campaign [15] and the average values of compressive strength of stone cubic samples (10 cm edge length) are presented in Table 1.

It is worth noting that in most of the old masonry buildings the binding material was air lime, since hydraulic lime was not used frequently, at least in Mediterranean countries, before the first decades of XX century. In this experimental programme masonry panels based on hydraulic lime were used to represent buildings which were built in later period and with the aim of comparing results with panels where air lime was used.

The hydraulic lime was produced by Secil Martingança Company. The air lime was prepared in the laboratory following the traditional preparation methodology: cooked lime stones were added slowly in a big barrel where the appropriate amount of water had been introduced, and boiled until air lime was obtained.

The two types of mortar used in the panel's construction, were made with a sand/binder ratio of 3/1, in volume, which is similar to the mix proportions of traditional mortars. The mortars mechanical properties, such as flexural and compressive strength, were obtained by experimental tests performed simultaneously with the diagonal compression tests.

Table 1
Compressive strength of stone cubic panels [15].

Cubes average values	Ultimate load (kN)	Compressive strength (MPa)
	478	48

For the flexural strength (mortar flexural strength is the mortar tensile strength obtained by bending tests), nine prismatic specimens (160 × 40 × 40 mm) were tested according to the EN 1015-11 standard [16] and the obtained mean value of the flexural strength is 0.35 MPa for the hydraulic mortar and 0.25 MPa for the air lime mortar. Compression tests were also performed and the obtained compressive strength was 1.47 MPa and 0.56 MPa for the hydraulic mortar and the air lime mortar, respectively.

The panels were built in the test position, and supported on the two lower faces during construction, as shown in Fig. 2. The first panel was constructed by applying the stones in horizontal layers, whereas the other three panels were built with diagonal stone layers. The intention was to obtain some insight to the influence of the stone arrangement on the shear strength and ductility of the panels.

According to the ASTM E519-02 standard [5] two steel loading shoes, with maximum length of bearing of 1/8 of the length of the specimen edge, were used. Namely, all panels were constructed on the bottom steel element (loading shoe) and before the test of the panel, in order to apply the load, other loading shoe was placed on the top of the panel. To avoid premature splitting and failure of panel edges, the space between the specimen and steel plates is filled with appropriate type of mortar.

It is important to say that all panels were built according to the traditional rules by an experienced mason.

3. Diagonal compression test

3.1. Test description

The diagonal compression test is carried out to determine the diagonal tensile (shear) strength and it is performed in square masonry panels that are tested with the diagonal in the vertical direction and compressed in that direction. The size of the panels is selected as the smallest to be reasonably representative and to allow the use of the usual testing machines. The ASTM standard recommends dimension of panels 120 cm × 120 cm, which was adopted in the present work. The thickness is 70 cm, the medium thickness of the external masonry walls of "Pombalino" and "Gaioleiro" buildings.

After construction, due to panel's size and to the nature of mortars which were used, air and hydraulic lime mortars, considering the different speed of hardness, the panels were not relocated from the original position and a curing period of 8 months was adopted.

The test setup is composed of two steel loading shoes (Fig. 3) placed on two diagonally opposite corners of the masonry panels. One of the loading shoes supports the panel and it is in contact with the laboratory slab, while the other one is placed on top of

Fig. 2. Evaluation of panels construction.

Fig. 3. Loading shoe.

the panels, where the 800 kN capacity hydraulic jack applies the vertical load (Fig. 4).

During testing, the vertical load was applied to the panel by a hydraulic jack acting on the top steel shoe and transmitted to the bottom shoe. The shortening of the vertical diagonal and the lengthening of the horizontal diagonal were measured with linear displacement transducers (TSV and TSH, respectively), which were placed on both sides of the masonry panels. The total number of channels used for each panel was eight (five transducers were installed on one side of the panel and three transducers were placed on the other side), as depicted in Fig. 5.

3.2. Interpretation of the diagonal compression test

One of the most used methodologies to evaluate the shear strength of masonry panels based on the results of diagonal compression tests is the one proposed on the ASTM specifications [5]. According to this the shear stress can be calculated as:

$$\tau = \frac{0.707 \times P}{A_n} \tag{1}$$

where P is the load applied by the jack and A_n is the net area of the panel, calculated as follows:

$$A_n = \left(\frac{w+h}{2}\right) \times t \times n \tag{2}$$

where w is the panel width, h is the panel height, t is the total thickness of the panel and n is percent of the unit's gross area that is solid, expressed as a decimal. In the present work $n = 1$ was adopted.

The shear strain γ is evaluated as:

$$\gamma = \frac{\Delta v}{g_v} + \frac{\Delta h}{g_h} \tag{3}$$

where Δv is the vertical shortening of the panel, Δh is the horizontal elongation of the panel, and g_v and g_h are the vertical and horizontal gage lengths (see Fig. 5a), respectively.

Consequently, the shear strength τ_0 (f_{vo} according to Eurocode 6 [17]) and the tensile strength f_t are defined as:

$$\tau_0 = f_t = \frac{0.707 \times P_{max}}{A_n} \tag{4}$$

where P_{max} is the maximum load applied by the jack.

The modulus of rigidity G (modulus of elasticity in shear) is obtained by:

$$G = \frac{\tau_{1/3}}{\gamma_{1/3}} \tag{5}$$

where $\tau_{1/3}$ is the shear stress for a load of 1/3 of the maximum load P_{max} and $\gamma_{1/3}$ is the corresponding shear strain.

This issue is further analyzed by using the semi-inverse method used in Strength of Materials. Some plausible hypotheses are used to characterize the stress field inside a homogenous panel under diagonal compression, and based on those hypotheses the shear stress in the wall is related to the applied load. The hypotheses regarding the stress field are the following: for square specimens ($h \times h$) it is admitted that at the horizontal diagonal, perpendicular to the load, (i) the vertical component of the stresses σ_v are equal to the applied load divided by the area, Eq. (6), and (ii) the stress vector is in the direction from each point located at a horizontal distance x from the center of the panel to the top corner where the load is applied, as shown in Fig. 6a, leading to the relation of the horizontal $\sigma_h(x)$ and vertical σ_v components of the stress as defined in Eq. (7).

$$\sigma_v = \frac{P}{h\sqrt{2} \times t} \tag{6}$$

$$\frac{\sigma_h(x)}{\sigma_v} = \frac{x}{h\sqrt{2}/2} \tag{7}$$

Therefore, at each point of the horizontal diagonal, the horizontal component of the stress (outwards) due to each of the applied forces P (at top and bottom of the specimen) is:

$$\sigma_h(x) = P\frac{x}{h^2 t} \tag{8}$$

The total horizontal force $N(x)$, due to both P forces, generated at a length dx of the diagonal is:

$$N(x) = 2\sigma_h(x)tdx = 2P\frac{x}{h^2}dx \tag{9}$$

Assuming that this force spreads at 45°, at the vertical diagonal it spreads along a length of $2x$ (Fig. 6b). Therefore the horizontal tensile stress $\sigma_H(x)$ in this zone of the vertical axis would be:

$$\sigma_H(x) = \frac{N(x)}{2xt} = \frac{P}{h^2 t}dx \tag{10}$$

Therefore at the intersection of the diagonals, where the tensile stress is higher, triggering cracking and rupture, the total tensile stress σ_t can be obtained by the sum of the contributions on each part of the horizontal diagonal, as follows:

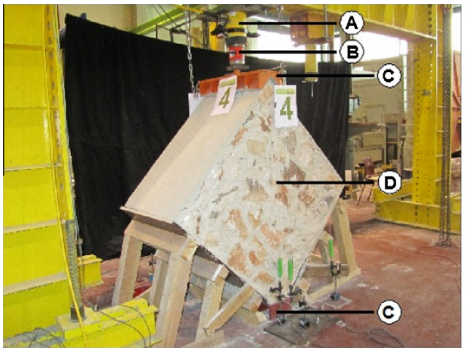

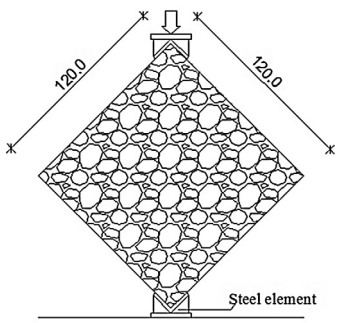

Fig. 4. Test setup for diagonal compression test (dimensions in [cm]). A – Hydraulic jack, B – load cell, C – loading shoes and D – masonry panel.

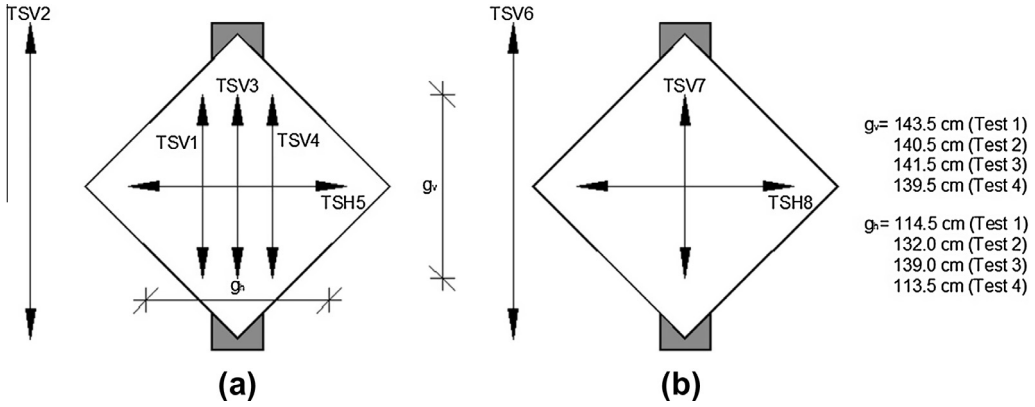

Fig. 5. Transducers position: (a) panel front side and (b) panel back side (dimensions in [cm]).

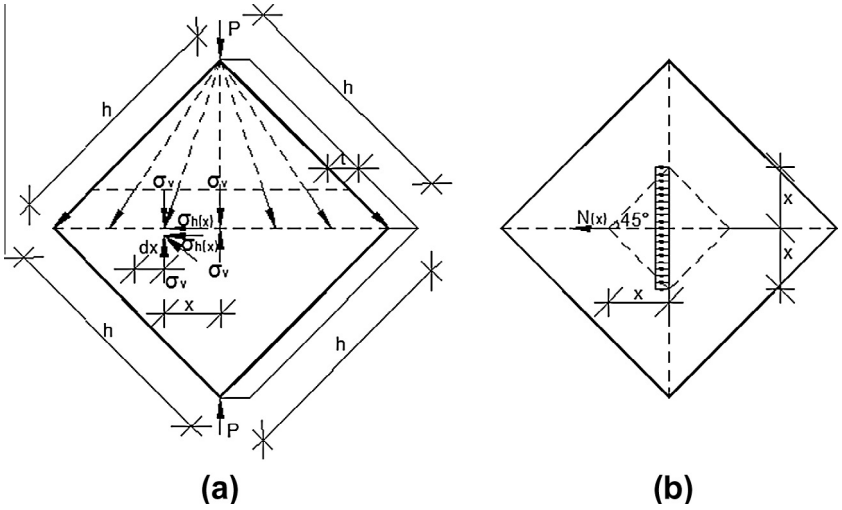

Fig. 6. Internal stresses on the specimens.

$$\sigma_t = \int_0^{h\sqrt{2}/2} \sigma_H(x) = \int_0^{h\sqrt{2}/2} \frac{P}{h^2 t} dx = \frac{P}{\sqrt{2}ht} = \sigma_v \tag{11}$$

In this case the Mohr's circle is centered in the origin in the Cartesian system of axis and the value of the shear stress τ is equal to the principal tensile stress σ_t, as shown in Fig. 7.

$$\tau = \sigma_v \tag{12}$$

Therefore, from Eqs. (6) and (12) the following expression is obtained

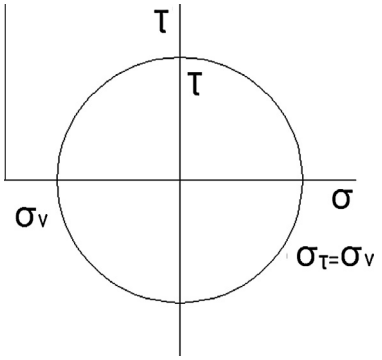

Fig. 7. Mohr's circle at the center of the specimen.

$$\tau = \sigma_v = \frac{P}{h\sqrt{2} \times t} = \frac{0.707 \times P}{A_n} \tag{13}$$

The methodology adopted in this work leads to the expression proposed by ASTM [5]. The experiments described in the next section confirm that the crack development at the panels effectively started at the center of the panel. Apparently this result is on the safe side as the value of τ derived in this way is the one associated with the initiation of cracking at the center of the panels, and at this situation the applied load was still slightly below the ultimate.

However, for non-homogenous masonry panels tested by diagonal compression some authors have recently proposed alternative equations to estimate the tensile strength f_t.

Brignolla et al. [9] modeled numerically diagonal compression tests and concluded that for irregular masonry panels, which are the current case, the prediction of tensile strength from the ASTM approach is unconservative. A new formula for the evaluation of the tensile strength of masonry based on the diagonal compression test was then proposed:

$$f_t = \frac{\alpha \times P}{A_n} \tag{14}$$

where α is a coefficient dependent on masonry typology. For irregular masonry the suggested value is $\alpha = 0.35$. The ASTM approach corresponds to $\alpha = 0.707$ whereas for the RILEM standard [18] α is equal to 0.5.

4. Experimental results

As already mentioned, the four masonry panels were constructed using two types of mortar, one based on hydraulic lime (panels W1 and W4) and the other based on air lime (panels W2 and W3). The diagonal compression tests on the four rubble masonry panels were characterized by similar failure patterns, as presented in Fig. 8. In all tests a main crack developed at the center of the panels, propagated along the vertical towards the upper and bottom corners of the panel and caused the collapse. This crack developed through the mortar with no damage on the stones and divided the panel in two almost symmetrical parts.

The panels collapse was fragile in all cases but, due to the mortars mechanical properties, the panels showed different behaviors at collapse. The air lime mortar panels, W2 and W3, disintegrated at collapse whereas in the case of hydraulic mortar panels, W1 and W4, each of the two broken parts remained almost in one piece (Fig. 9).

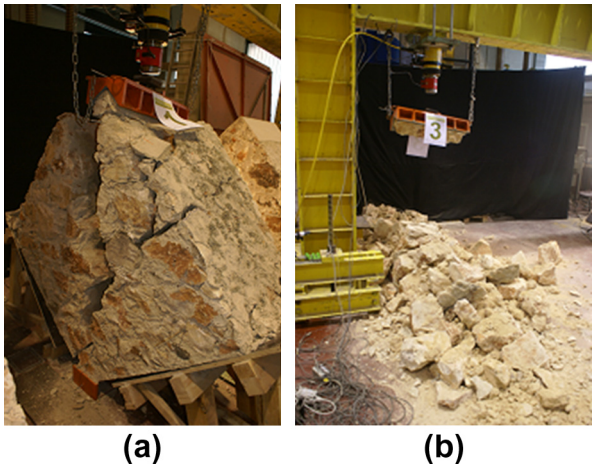

Fig. 9. Collapse of masonry panels: (a) panel W1 made with hydraulic mortar; and (b) panel W3 made with air lime mortar.

4.1. Masonry panels with hydraulic lime mortar

The experimental results for the diagonal compression tests on the hydraulic lime mortar panels are depicted on Fig. 10, where the load-vertical displacement diagram is represented, (vertical displacement represents the average value of the measurements recorded using LVDTs 3 and 7). As it is shown on this graphic the maximum load for panel W1 was 372 kN (Point 1), with a vertical shortening of 1.55 mm. The collapse occurred later, with a vertical shortening of 5.29 mm and a load of 268 kN (Point 2). In panel W4 the maximum load applied was at the point of collapse, with a magnitude of 306 kN (Point 3) and a vertical displacement of 3.47 mm. It is worth noting, that this apparent "ductile" behavior of panel W1 is related to the stone arrangement, since the panel W1 was built with horizontal stone layers, (at 45° to the external inclined surfaces), whereas the other three panels were built with diagonal layers (45°), to be representative of the real masonry walls.

It is worth to note that, for safety reasons, all transducers (except the transducer placed under the hydraulic jack) were removed before the end of the test. The dotted parts of the curves in Fig. 10 were obtained using the measurements of the transducers under the hydraulic jack, instead of the averages values of the two measurements.

The behavior of the tested panels can also be analyzed in terms of shear stress–shear strain curves, as presented in Fig. 11, where the shear stress and shear strain were calculated according to ASTM standard [5]. The shear strength, the modulus of rigidity and the tensile strength of panels from diagonal compression test, evaluated according to Section 3.2, are presented in Table 2.

4.2. Masonry panels with air lime mortar

The masonry panels built with air lime mortar showed much lower strength and deformation capacity than the hydraulic mortar panels. Collapse load for panel W2 was 29 kN (Point 1), with a vertical shortening of 1.58 mm, as it is shown in Fig. 12, and for panel W3 was 28 kN (Point 2), with a vertical displacement of 1.52 mm, where the vertical displacement were obtained as average values of the measurements recorded using LVDTs 3 and 7 for both panels.

As in the previous case, the transducers were removed before the end of the test (except the transducer that was placed under the hydraulic jack) and the dotted part of the lines in Fig. 12 were obtained using the measurement of the transducers under the hydraulic jack.

The similarity of these results, on panels W2 and W3 with the same stone arrangement, and the difference between the previous results, on panels W1 and W4 with different stone arrangements, show that the different stone arrangements lead to different strengths and very different deformation capacities on masonry panels.

The results of the diagonal compression tests in masonry panels W2 and W3 (shear strength, modulus of rigidity and tensile

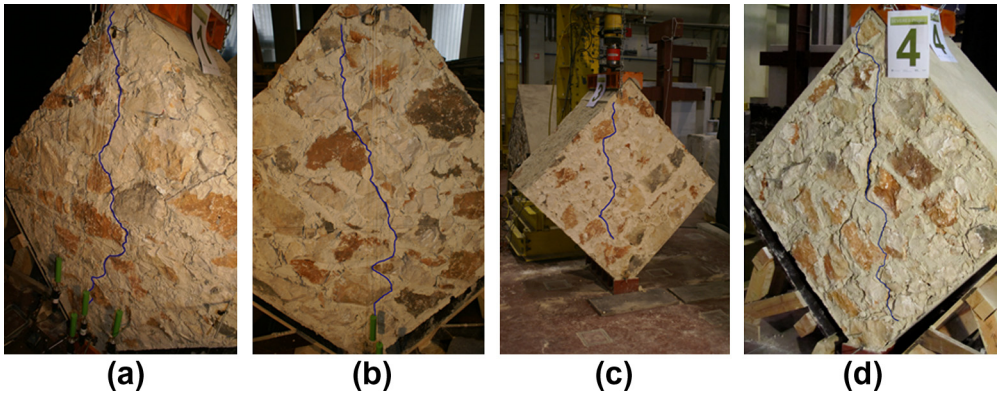

Fig. 8. Main crack at the middle of the panels before rupture: (a) and (d) panels made with hydraulic mortar (W1 and W4); (b) and (c) panels made with air lime mortar (W2 and W3).

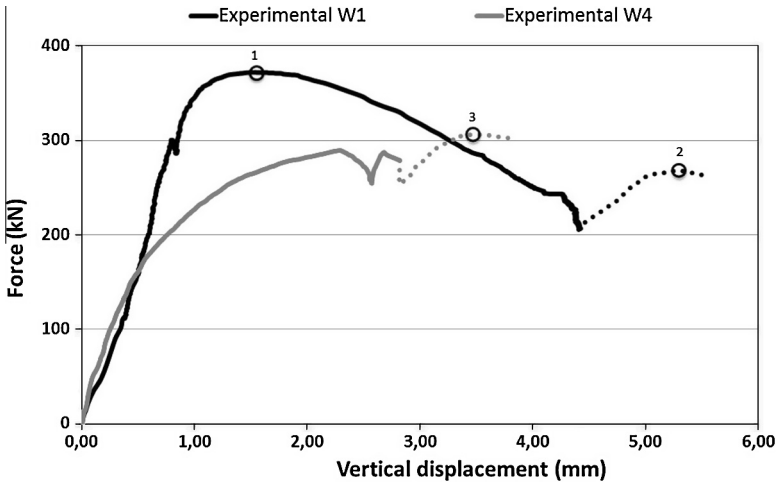

Fig. 10. Experimental results – panels W1 and W4: force vs. vertical displacement (*Note*: the dotted lines represent the vertical displacement extrapolated from the reading at the top of the specimen).

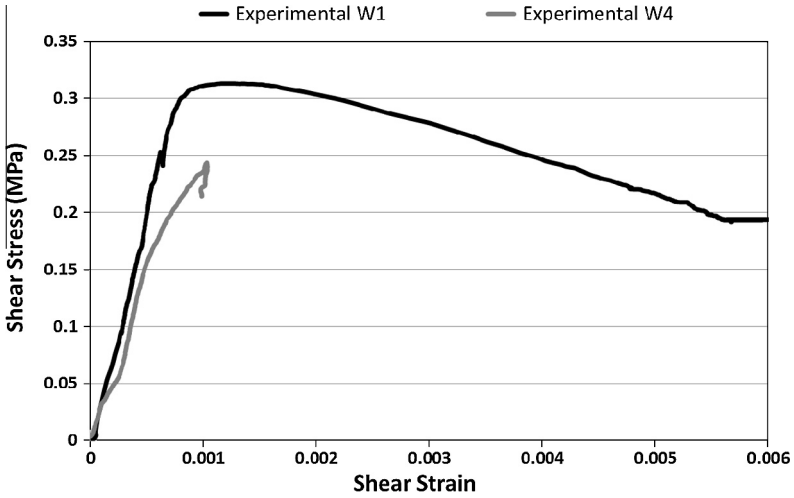

Fig. 11. Experimental results – panels W1 and W4: shear stress vs. shear strain (*Note*: for safety reason in wall W4 the transducers TSV1, TSV3, TSV4, TSV7, TSH5 and TSH8 were removed before the end of the test).

Table 2
Diagonal compression tests.

Masonry typology	Masonry panel	P_{max} (kN)	ASTM		RILEM	Brignola et al. [9]
			$\tau_0 = f_t$ (MPa)	G (GPa)	f_t (MPa)	f_t (MPa)
Rubble stone masonry panels	W1	372	0.313	0.389	0.220	0.155
	W2	29	0.024	0.058	0.017	0.012
	W3	28	0.024	0.093	0.017	0.012
	W4	306	0.258	0.252	0.182	0.128

strength, evaluated according to paragraph 3.2) are given in Table 2 and the corresponding shear stress–shear strain curves are depicted in Fig. 13.

4.3. Analysis and comparison of results

In Table 2 are summarized the results obtained with the diagonal compression tests and the corresponding strength values obtained by means of the three procedures mentioned in Section 3.2.

Based on the results obtained it can be concluded that the stone arrangement leads to some differences in masonry strength but especially on the deformation capacity. However the influence of stone arrangements is not as important as the influence of the type of mortar, which is very high: panels with air lime mortar exhibited shear strength below 10% of the shear strength of the panels built with hydraulic lime mortar. Note that this huge difference between the strength of panels made with air and hydraulic lime is not so pronounced in compression tests, where small strength differences usually occur [15].

The first conclusion from the experimental results is that the panel shear strength is strongly dependent on the mortar resistance, since the cracks propagated through the joints, without damaging the stones. The masonry panels built with air lime mortars showed a very low shear resistance.

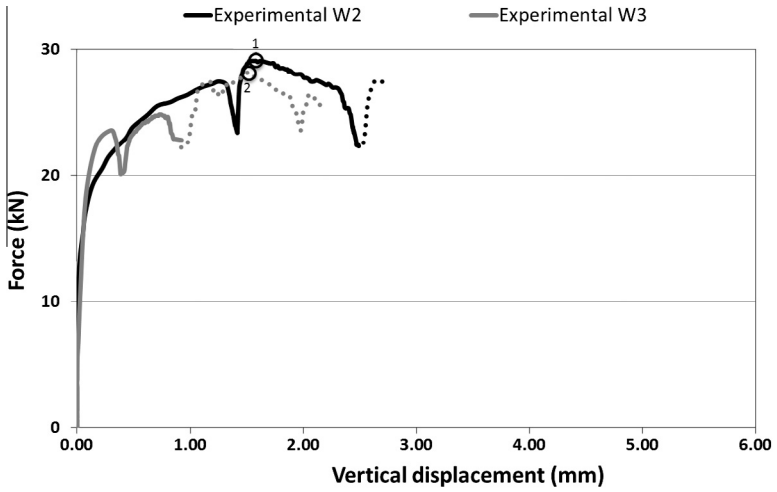

Fig. 12. Experimental results – panels W2 and W3: force vs. vertical displacement (*Note*: the dotted lines represent the vertical displacement extrapolated from the reading at the top of the specimen).

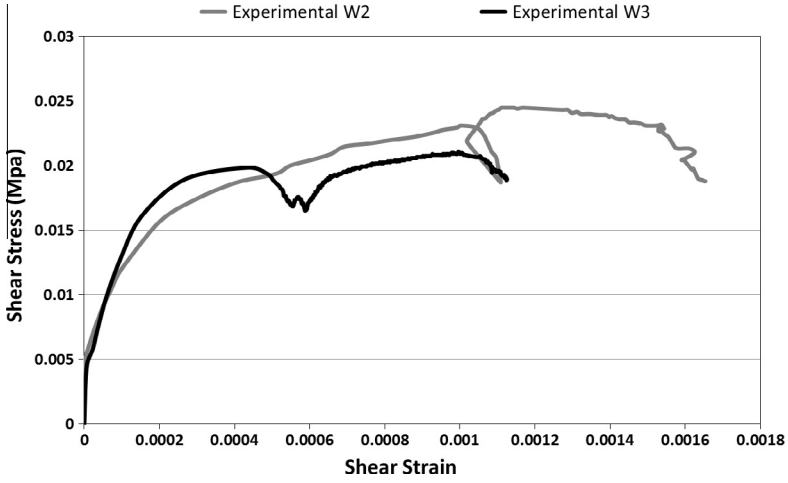

Fig. 13. Experimental results – panels W2 and W3: shear stress vs. shear strain.

Table 3
Diagonal compression (in situ) tests – literature review.

Traditional masonry (lime mortar and calcareous stone)	$f_t = \alpha \times P/A_n$		Shear modulus G (GPa)	
	α	f_t (MPa)		
Double-leaf roughly cut stone masonry	0.707	0.05–0.07	0.019–0.060	Corradi et al. [7]
Random rubble stone masonry	0.707	0.06–0.16	0.036–0.285	Chiostrini et al. [19]
Random rubble stone masonry	0.35	0.02–0.04	–	Brignola et al. [9]
Double-leaf roughly cut stone masonry	0.707	0.02–0.04	0.030–0.055	Borri et al. [12]
Triple-leaf roughly cut stone masonry	0.707	0.02–0.04	0.024–0.102	Borri et al. [12]
Random rubble stone masonry	0.5	0.04–0.07	0.301–3.917	Brignola et al. [10]
Rubble stone masonry	0.707	0.024	0.058–0.093	Current work (2011)

In addition, the values for tensile strength obtained by diagonal compression tests (Table 2) are much lower than the values obtained for the mortars tensile strength by bending tests (0.35 and 0.25 MPa for hydraulic and air lime mortars, respectively) and the relative differences between the tensile strength of hydraulic and air lime mortar specimens is much more marked in the diagonal compression tests. This can be due to the fact that the phenomena that conditions rupture are different in both cases: in the flexural test it is the tensile strength of the mortar and in the case of the diagonal compression test it is the tensile resistance of the interface between the mortar and the stones.

The obtained values for the shear elastic modulus G were measured in the elastic regime (1/3 of the maximum load) and the results also vary depending on the type of mortar (Table 2).

For masonry panels made with air lime mortar the measured values for G present a variation of 38%, with values of 0.058 GPa and 0.093 GPa for panels W2 and W3, respectively. In the tests of the masonry panels with hydraulic lime, considerable differences were also found: 0.389 GPa (panel W1) and 0.252 GPa (panel

W4), which is explainable by the stone arrangement of the masonry panel W1, built with horizontal layers.

The masonry panels made with air lime mortar showed a shear elastic modulus smaller than the shear elastic modulus obtained for the panel made with hydraulic lime mortar. However, the difference in relative terms is smaller than the difference obtained in the shear strength, which is explained by the fact that shear modulus G is evaluated on the undamaged panel with small displacements, where measurement errors may have an important influence.

Table 3 summarizes some selected results which were already published in the literature referring to the shear strength and shear modulus by other experimental campaigns where diagonal compression tests were also performed. It can be noticed, that the values of the shear strength for air lime mortar and shear modulus obtained in the current experimental research are comparable with the values from the literature.

It is worth note that most experimental results available in the literature indicate values of the masonry shear strength above the ones derived in the experimental campaign described in this paper using the ASTM proposed formulae, based on the value $\alpha = 0.707$. This points to the fact that this methodology yields acceptable conservative results for the shear strength, the alternatives being even more conservative.

5. Numerical modeling

Experimental tests provide values for mechanical parameters, but those values cannot be directly used in numerical modeling. A calibration process should be done in order to validate the values adopted for the mechanical parameters as well as the numerical models. This calibration process is particularly important when nonlinear material behavior is to be simulated, which is often the case of seismic structural studies on old masonry buildings [20].

There is little information about old masonry buildings mechanical parameters, but even less with regard to its use in numerical models. In the present work two types of numerical models were built to simulate the diagonal compression tests described in previous paragraphs: nonlinear finite element models [13] and distinct element models [14].

In the finite element models the cracking of masonry (the most important source of non-linear behavior) was simulated by a smeared crack approach. In the case of rubble stone masonry walls, where the location of potential cracks cannot be defined in advance, a smeared model seems to be preferable and more applicable for engineering practice than a distinct crack approach. However, it should be noticed that when the complete material degradation is to be modeled, smeared crack models are more unstable than distinct crack models.

The distinct elements method was primary developed for rock mechanics, but its numerical robustness and its properties, namely in the simulation of the interaction between elements (or blocks), make the method also attractive for modeling masonry structures. The distinct element method allows the explicit modeling of stones and mortar joints, with displacements and rotations of the individual blocks, and, thus, the simulation of masonry panel's failure mechanisms. The use of Voronoi algorithm [21] for elements (blocks) generation allowed reproducing the arbitrary stone arrangements in the masonry panels and made possible the use of distinct element method for rubble stone masonry panels.

5.1. Nonlinear finite element model

The adopted methodology for modeling the masonry panels by the finite element method required the use of nonlinear models to simulate the masonry non tension resistance. A smeared crack model (Total Strain Crack Model – [13]) based on a fixed stress–strain concept was used. In this model the stress–strain relations are evaluated in a local coordinate system which is fixed upon cracking. In others words, the crack orientation is kept constant during the whole computation process, which is physically realistic in the current case of study. Nonlinear geometric effects were not considered in the numerical simulations and eight-node isoparametric plane stress elements were used in the mesh generation (Fig. 14).

The smeared crack models are defined through the combination of three factors: (1) a tension cut-off failure criterion (constant or linear), (2) the shear transfer through the crack (total, constant or variable shear retention) and (3) the material softening behavior (brittle, linear, multilinear or non-linear). In the present work a constant tension cut-off criterion was used together with an exponential constitutive law for the softening behavior. For the shear behavior it was adopted constant shear retention (where the shear stiffness was reduced in the crack surface to 10% after cracking) and for the compressive behavior an elastic linear constitutive law was used.

The finite elements mechanical properties for both type of panels, namely the density ρ, Young modulus E, Poisson's ratio ν, tensile strength f_t, fracture energy G_{f1} and shear retention factor β, are presented in Table 4. For density, Poisson's ratio and fracture energy typical values adopted in other numerical works [4,22–24] were considered.

For the shear retention factor, a parameter associated with the shear transference across cracks, the used value was obtained by calibration of the experimental and numerical results. The adopted value ($\beta = 0.1$) is a current value used in the simulation of the cracked plain concrete behavior, but is slightly larger than the value used by Rots et al. [22] and Ramos and Lourenço [23]. However the adopted value is coherent with the experimental evidence where the interlocking of the stones allows to an important shear transference after crack occurrence.

The Young's modulus and tensile strength were also quantified by calibration of the numerical and experimental results. With

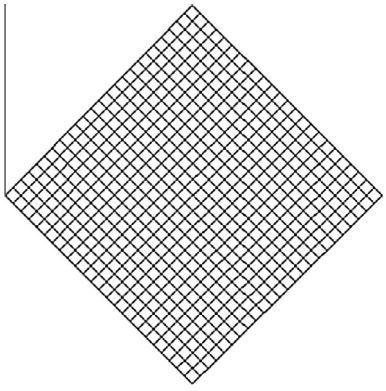

Fig. 14. Finite element model mesh.

Table 4
Mechanical properties for numerical analysis with finite element method.

Masonry panel	Density ρ (kg/m^3)	Young modulus E (GPa)	Poisson's ratio ν	Tensile strength f_t (MPa)	Fracture energy G_{f1} (Nmm/mm^2)	Shear retention factor β
W4	1835	3.27	0.20	0.15	0.1	0.1
W2	1835	3.27	0.20	0.01	0.1	0.1

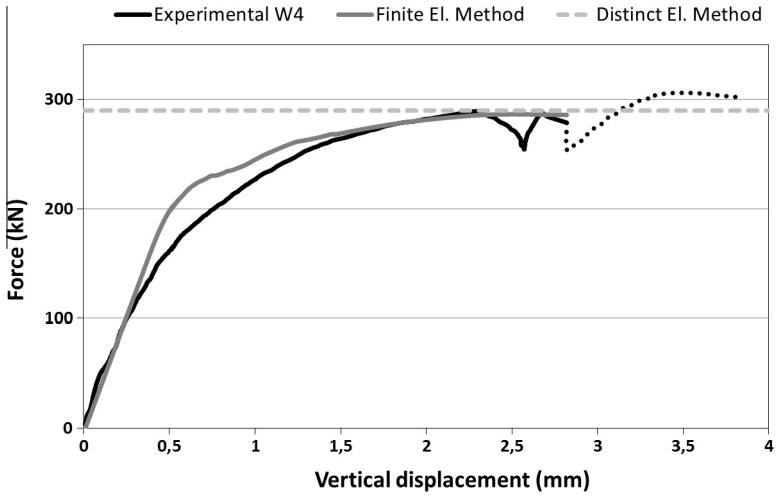

Fig. 15. Numerical & experimental results: force vs. vertical displacement diagram for panel W4.

those results, which are not far from the typical values, a good match was obtained.

The vertical load was applied monotonically at the top of the panel, as in the experiments, and a displacement controlled procedure was applied to impose the load up to failure, using the regular Newton–Raphson iteration procedure.

Considering the results obtained with the finite element method, which can be seen on Figs. 15 and 16, an acceptable matching between numerical and experimental values for both the ultimate load and the initial loading branch are obtained. The damages observed in the numerical model are also coherent with the observed collapse during the experimental tests, as can be seen on Fig. 17a

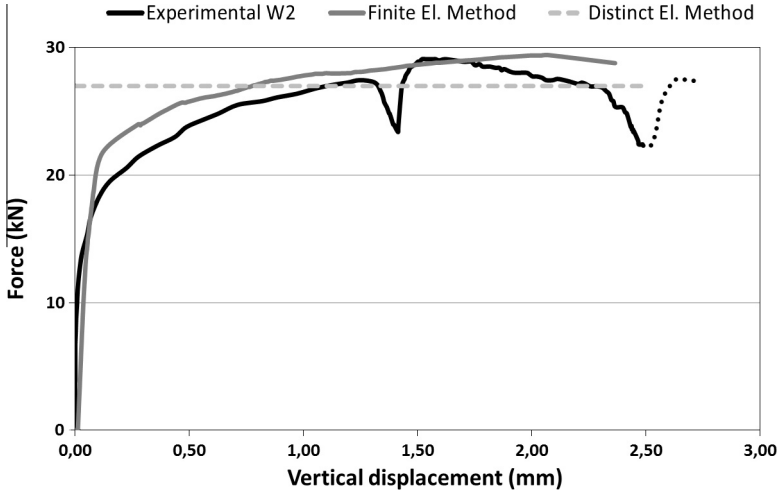

Fig. 16. Numerical & experimental results: force vs. vertical displacement diagram for panel W2.

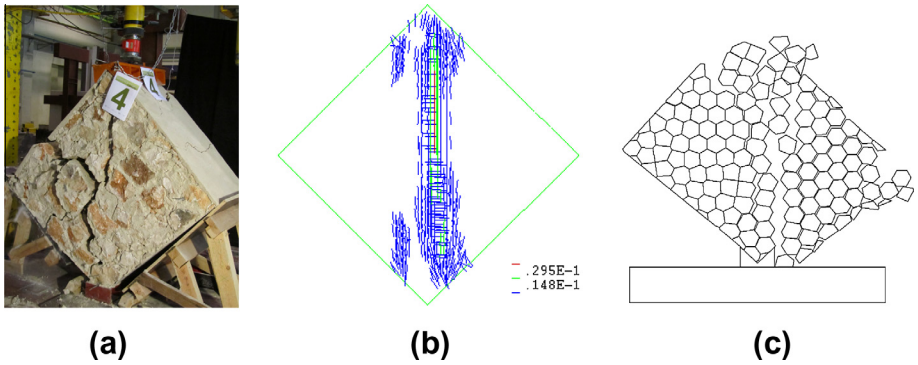

Fig. 17. Panel W4 – experimental and numerical failure modes: (a) Experimental, (b) finite element model and (c) distinct element model (the picture shows the panel immediately before the complete collapse).

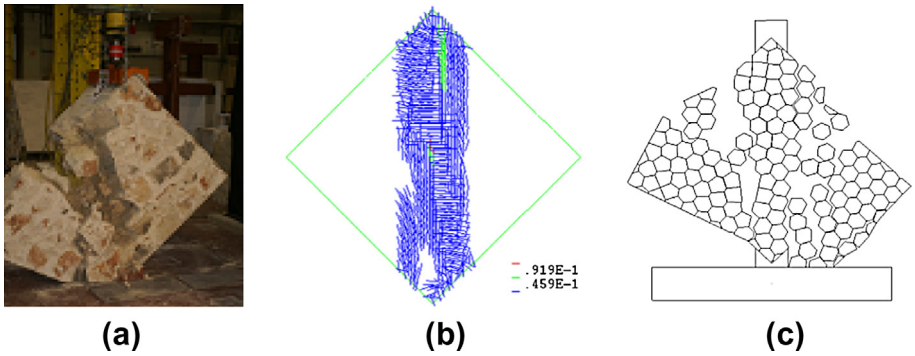

Fig. 18. Panel W2 – experimental and numerical failure modes: (a) Experimental, (b) finite element model and (c) distinct element model (the picture shows the panel immediately before the complete collapse).

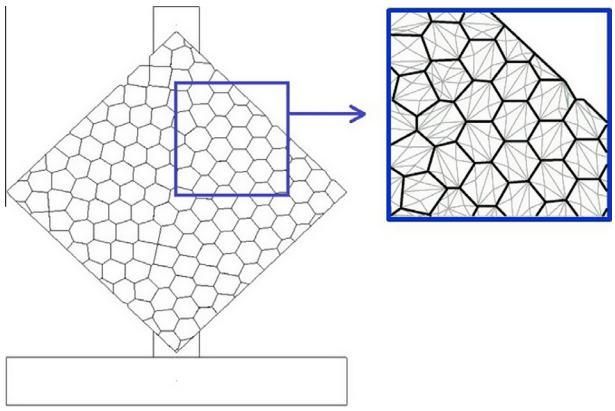

Fig. 19. Randomly sized polygonal blocks.

Table 5
Mechanical properties for numerical analysis with distinct element model.

Masonry panel	Bulk modulus K (GPa)	Shear modulus G (GPa)	Normal stiffness J_{kn} (GPa)	Shear stiffness J_{ks} (GPa)	Friction angle ϕ (°)	Cohesion c (MPa)	Tensile strength f_t (MPa)
W4	0.41	0.45	17	17	45	0.23	0.23
W2	0.41	0.45	8	8	45	0.03	0.03

and b for hydraulic lime mortar and Fig. 18a and b for air lime mortar. Figs. 15 and 16 also show the ultimate load obtained by the distinct element method referred in Section 5.2.

5.2. Distinct element model

As mentioned, the distinct element models of the masonry panels consisted in a group of randomly sized polygonal blocks generated by an automatic joint generator (Fig. 19). Each block simulates a stone and was modeled by a finite difference elements mesh (Fig. 19) with linear elastic behavior (bulk modulus K and shear modulus G). In addition, an appropriate behavior was assigned to the contacts between the blocks using a Coulomb slip model. The parameters that control the contact behavior are the normal stiffness J_{kn} the shear stiffness J_{ks}, the friction angle ϕ, the cohesion c and the tensile strength f_t. The joint deformability parameters J_{kn} and J_{ks} control the initial loading branch and the joint strength parameters ϕ, c and f_t control the ultimate force level. The normal and shear stiffness are used to model the deformability of the mortar and blocks in the vicinity of the contact joint. Table 5 presents the adopted values for these parameters for the two cases: air lime mortar and hydraulic lime mortar panels. Those values were quantified based on values adopted in other works [24–27] and the calibration of the numerical and experimental results.

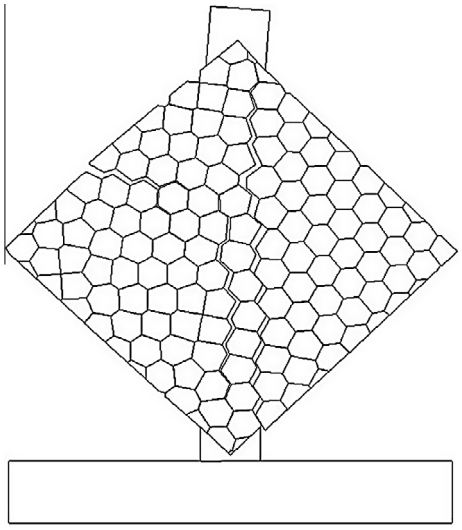

Fig. 20. Main crack obtained by the distinct element model – panel W4.

The numerical results obtained with the distinct element model for panels made with hydraulic and air lime mortar can be seen in Figs. 15 and 16, respectively, and the corresponding collapse mode for both type of mortar is depicted in Figs. 17c and 18c, respectively. In Fig. 20 is depicted the main crack obtained on the distinct element simulations, which is similar to the crack observed in the experimental tests (Fig. 8). As it can be seen in those figures a good matching between numerical and experimental values was achieved for the ultimate load and for the collapse pattern.

5.3. Discussion

A general overview of the results obtained in the numerical analysis was presented, where force displacement diagrams and failure modes were some of the aspects under analysis. An acceptable matching between numerical and experimental results for the ultimate load and collapse modes can be noted for both, finite element and distinct element models. As shown in Figs. 17, 18 and 20, the obtained crack patterns (diagonal cracking) in the numerical models were quite similar to the ones obtained in the experimental tests.

A good agreement with experimental results was also obtained in the finite element analysis for the initial branch of the load–dis-

placement curve. In the distinct element analysis this curve cannot be obtained directly (since equilibrium is established for full loads and not at load increments), which represents a clear advantage of the finite element method. However, modeling with finite element models was much more demanding in the sense that the numerical convergence required a continuous review of the convergence criteria.

Since the location of the potential cracks are unknown in rubble stone masonry, the smeared crack approach is more appropriate for modeling large rubble stone masonry panels than the distinct crack approach or the distinct element method. However, the use of the Voronoi algorithm to randomly generate the blocks in the distinct element model allows the use of a distinct methodology in a smeared sense.

6. Conclusions

For the structural assessment of old buildings with load bearing masonry walls and for the eventual design of strengthening solutions it is required an accurate simulation of its structural behavior. For this it is essential to know the materials mechanical characteristics, which is not always possible due to the lack of experimental data. For the seismic assessment, where the shear behavior of masonry walls is an extremely important aspect, the difficulties are even greater because there are very few data on the shear strength of rubble stone masonry walls. This work aims to contribute to fill this gap, evaluating of the shear strength for traditional rubble stone masonry panels via diagonal compression tests.

Masonry panels were specially built for the experimental program using materials and the techniques similar to what was used in old buildings. Four 1.20 m × 1.20 m × 0.7 m panels were built and tested – two with air lime mortar and two with hydraulic lime mortar.

The tested masonry panels showed a fragile behavior with low values of shear strength, especially in the case of the models made with air lime mortar ($\tau_{0,ASTM}$ = 0.024 MPa), as the panels with hydraulic mortar reached $\tau_{0,ASTM}$ = 0.313 MPa and $\tau_{0,ASTM}$ = 0.258 - MPa. It was noted that the mortar composition (air or hydraulic lime) has an important influence on shear strength. The tests showed also that an appropriate stone arrangement can increase the ductility of the panel. It can be noticed that the experimental results for shear strength obtained for panels with air lime mortar and calculated according to the ASTM procedure ($\tau_{0,ASTM}$ = 0.024 - MPa) are close to the values of the Italian's Standard [28] (τ_0 = 0.02 MPa to 0.032 MPa).

The tests were numerically simulated by nonlinear finite elements models (smeared crack concept) and distinct elements models, which demonstrated their ability to simulate the masonry behavior in shear. Both numerical procedures gave results with a good matching to the experimental results and the collapse patterns were similar to the experimental ones. With the finite elements models the complete load–displacement curve was obtained, whereas with the distinct element method only the maximum applied load can be achieved. However, it must be noted that in order to obtain convergence in all analysis steps, the finite element models required much more attention from the operator than in case of distinct elements models. The simulation of rubble stone masonry panels by the distinct element method was achieved due to the use of the Voronoi algorithm in the blocks generation.

Acknowledgments

The authors acknowledge the financial contribution of the FCT (*Fundação para a Ciência e a Tecnologia*) project SEVERES: "Seismic Vulnerability of Old Masonry Buildings". The work was carried out at the *Instituto de Engenharia de Estruturas, Território e Construção* (ICIST), using the laboratory and computational facilities of the Department of Civil Engineering, *Architecture and Georesouces of Instituto Superior Técnico* (IST) in Lisbon, Portugal.

References

[1] ICOMOS: recommendations for the analysis, conservation and structural restoration of architectural heritage. ICOMOS, International scientific committee for analysis and restoration of structures of architectural heritage; 2003.
[2] Cardoso R, Lopes ML, Bento R. Seismic evaluation of old masonry buildings. Part I: Method description and application to a case-study. Eng Struct 2005;27:2024–35.
[3] Bento R, Lopes ML, Cardoso R. Seismic evaluation of old masonry buildings. Part II: Analysis of strengthening solutions. Eng Struct 2005;27:2014–23.
[4] Mendes N, Lourenço PB. Seismic assessment of masonry "Gaioleiro" buildings in Lisbon, Portugal. J Earthq Eng 2010;14:80–101.
[5] ASTM: ASTM E 519-02 standard test method for diagonal tension (Shear) in masonry assemblages. ASTM International, West Conshohocken, PA; 2002.
[6] Corradi M, Borri A, Vignoli A. Strengthening techniques tested on masonry structures struck by the Umbria-Marche earthquake of 1997–1998. Constr Build Mater 2002;16:229–39.
[7] Corradi M, Borri A, Vignoli A. Experimental study on the determination of strength of masonry walls. Constr Build Mater 2003;17:325–37.
[8] Corradi M, Tedeschi C, Binda L, Borri A. Experimental evaluation of shear and compression strength of masonry wall before and after reinforcement: deep repointing. Constr Build Mater 2008;22:463–72.
[9] Brignola A, Frumento S, Lagomarsino S, Podestà S. Identification of shear parameters of masonry panels through the in-situ diagonal compression test. Int J Archit Heritage 2008;3:52–73.
[10] Brignola A, Podestà S, Lagomarsino S. Experimental results of shear strength and stiffness of existing masonry walls. New Delhi: Structural Analysis of Historical Constructions; 2006.
[11] Borri A, Castori G, Corradi M. Shear behavior of masonry panels strengthened by high strength steel cords. Constr Build Mater 2010;22:463–72.
[12] Borri A, Castori G, Corradi M, Speranzini E. Shear behaviour of unreinforced and reinforced masonry panels subjected to in situ diagonal compression tests. Constr Build Mater 2011;25:4403–14.
[13] DIANA: DIsplacement method ANAlyser, release 9.1 [CD–ROM]. Delft, The Netherlands: TNO DIANA BV; 2005.
[14] ITASCA: UDEC version 4.01 – User's guide. Itasca Consulting Group, Inc., Minneapolis, USA; 2011.
[15] Carvalho J. Mechanical characterization of loadbearing masonry stone through non-destructive testing. Master's thesis, Instituto Superior Técnico, Lisbon; 2008 [in Portuguese].
[16] CEN: 1015-11, 1999. Methods of test for mortar for masonry – Part 11: Determination of flexural and compressive strength of hardened mortar; 1999.
[17] EC 6: Eurocode 6 Design of masonry structures. Part 1 – 1: General rules for buildings – rules for reinforced and unreinforced masonry 1995. ENV 1996-1-1; 1995.
[18] RILEM TC.: 76-LUM Diagonal tensile strength tests of small wall specimens. In: RILEM, recommendations for the testing and use of constructions materials. London: E& FN SPON; 1994. p. 488–9.
[19] Chiostrini S, Galano L, Vignoli A. On the determination of strength of ancient masonry walls via experimental tests. In: Proceedings of the twelfth world conference on earthquake engineering (CD-ROM), Auckland, New Zealand; 2000. Paper No. 2564.
[20] Lourenço PB. Computations on historic masonry structures. Prog Struct Eng Mater 2002;4–3:301–19.
[21] Klein R. Concrete and abstract voronoi diagrams. Lecture notes in computer science. Springer-Verlag, vol. 200; 1989.
[22] Rots JG, Belletti B, Boonpichetvong M, Invernizzi S. Event by event strategies for modeling amsterdam masonry structures. Structural analysis of historical constructions, New Delhi; 2006.
[23] Ramos LF, Lourenço PB. Advanced numerical analysis of historical centers: a case study in Lisbon. Eng Struct 2004;26:1295–310.
[24] Gago AS. Análise Estrutural de Arcos, Abóbadas e Cúpulas – Contributo para o estudo do património construído (in portuguese), PhD Thesis, Faculty of Engineering, IST-UTL Tecnhical University of Lisbon, Lisbon; 2004. <http://www.civil.ist.utl.pt/~gago/Artigos/tese_PhD_ASGago.pdf>.
[25] Gago AS, Alfaiate J, Lamas A. The effect of the infill in arched structures: analytical and numerical modeling. Eng Struct 2011;33–5:1450–8.
[26] Azevedo J, Sincraian G, Lemos JV. Seismic behavior of blocky masonry structures. Earthq Spectra 2000;16–2:337–65.
[27] Lemos JV. Discrete element modeling of the seismic behavior of stone masonry arches. In: Pande GN, Middleton J, Kralj B, editors. Computer methods in structural masonry – 4. E & FN Spon, London; 1998. p. 220–7.
[28] NTC08. Ministero delle Infrastrutture e dei Transporti – Nuove Norme Tecniche per le Costruzioni. Italian Ministry of Infrastructures and Transportation, G.U. n.29 – S.O. n.30, February, 4th 2008, Rome, Italy; 2008 [in Italian].